Study on Hydrogen Embrittlement Susceptibility of 20# Pipeline Steel Welded Joint by Hydrogen-Doped Tensile Test

Xu Wang, Xiang Chen*[1], Jingyu He, Nianqi Chen
*School of Materials Science and Engineering, Tsinghua University, Beijing,100084, People's Republic of China, China

ABSTRACT.

The sensitivity of 20# pipeline steel in gaseous hydrogen environment was evaluated by slow strain rate tensile experiment. The variation of hydrogen embrittlement sensitivity of 20# pipeline steel with hydrogen content was studied. The results show that the tensile strength of hydrogen embrittleness sensitivity index increases gradually, the section shrinkage rises gradually, and the dimple decreases gradually with the increase of hydrogen blending ratio (5%, 15%, 25% and 100%). 105 °C is the maximum temperature for the 20# steel hydrogen trap. The possible gas products in hydrogen embrittlement were calculated by thermodynamics.

Keywords: Hydrogen blended natural gas; 20# pipeline steel; welded joint; Hydrogen embrittlement; Hydrogen blending ratio; Tensile test

1. INTRODUCTION

With the scarcity of fossil fuels and the deterioration of the global environment, renewable clean energy sources such as wind, solar, geothermal, and tidal energy are receiving increasing attention[1]. However, the instability and periodicity of renewable energy seriously constrain its development and may result in significant energy waste[2][3]. The technology of producing hydrogen through electrolysis of water converts renewable energy into hydrogen, and uses hydrogen as an energy carrier for storage and transportation, providing an effective way to solve the above problems[4-7]. The construction of new hydrogen transportation infrastructure and pipelines has led to high costs, which has constrained the development of hydrogen energy in the energy supply system[8]. As an emerging technology, incorporating hydrogen into existing natural gas pipelines can achieve large-scale hydrogen transportation at lower costs and is receiving increasing attention[9-13].

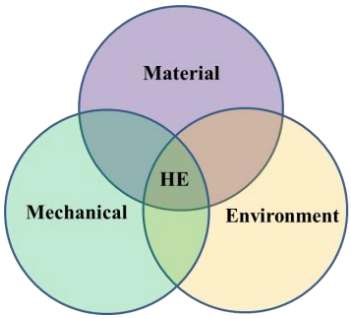

Figure.1. Factors responsible for hydrogen embrittlement[14]

HE of steel pipes involves environmental, material and mechanical factors[14], as shown in Figure 1. The interaction between these factors leads to various HE consequences of pipeline steel. The purpose of this study is to evaluate the hydrogen embrittlement specific resistance of pipeline steel X70 and to help deepen the understanding of the effect of hydrogen on medium and low strength steels. Although the mechanism of hydrogen embrittlement is a topic of

[1*]xchen@tsinghua.edu.cn

The International Conference Optoelectronic Information and Optical Engineering (OIOE2024), edited by Yang Yue, Lu Leng, Proc. of SPIE Vol. 13513, 1351327 · © 2025 SPIE · 0277-786X · © The Authors. Published under a Creative Commons Attribution CC-BY 3.0 License · doi: 10.1117/12.3045665

numerous studies[15-21], it is currently unclear how to choose which mechanism is the most active among them. This article studies the mechanical properties of 20# pipeline steel.

2. EXPERIMENTAL STUDY

The material of the study was a low strength steel grade 20# which chemical composition was given in Table 1. It is received as a part of the pipeline, and the sample is processed in the area near the weld. Because the axial direction can better reflect the tensile condition of steel, that is, along the direction of the pipeline, a smooth axisymmetric tensile specification is processed.

Table 1-Chenical composition of 20# pipeline steel (wt%).

Element	C	Si	Mn	P	S	Al
20#	0.20	0.24	0.45	≤0.020	≤0.010	0.010

Custom-made experimental setups were used to conduct corrosion experiments and tensile strength tests, as shown in Figure 2a. Tensile strength testing (TST) apparatus was utilized to evaluate the mechanical properties of the materials after exposure to the corrosive environment. Before conducting the tensile strength test, the specimens were exposed to the corrosive environment[39-41]. The sample after the experiment is shown in Figure 2b.

Figure.2a .The test TST apparatus diagram of the test setup

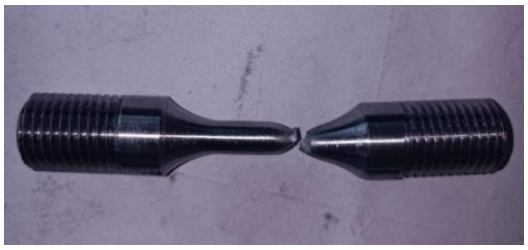

Figure. 2b. Sample after tensile test

3. RESULTS AND DISCUSSION

In the first set of experiments, the smooth sample was subjected to a tensile test in a hydrogen gas (H2 test) with a different ratio of 4 MPa and a strain rate of $2 \times 10-5\ s-1$. Each experiment is conducted twice, and the results are repeatable. Figure 3 shows representative results, emphasizing the influence of hydrogen on the yield stress and ultimate tensile stress of steel, as well as the strain hardening step before necking. On the contrary, the failure strain is greatly reduced, which means that most of the hydrogen effect is concentrated in the last part of the curve[42-45].

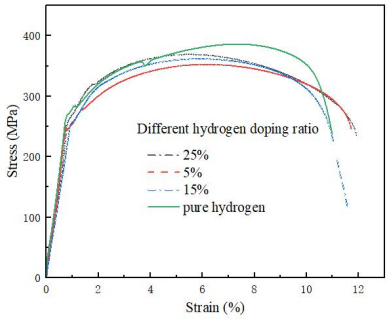

Figure. 3 .Stress-strain curves of 20# pipeline steel with different hydrogen blending ratios.

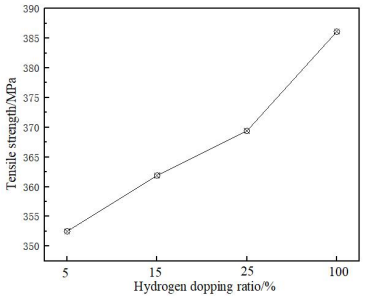

Figure. 4 Tensile strength of 20# pipeline steel with different hydrogen blending ratios.

The part of the stress-strain curve is zigzag, which indicates that in this environment, there is local instability in the specimen during deformation strengthening, and the deformation during stretching mainly occurs in the form of slip or double deformation [45-47]. When the slip or double strain rate, that is, the local plastic deformation rate exceeds the motion speed of the testing machine chuck, the local stress relaxation will be caused. The curve is clearly divided into three stages. The first stage is the micro-deformation stage, that is, the work hardening stage, the plastic deformation has just begun, the stress has risen linearly, the work hardening rate is high, the dynamic recovery has not been carried out, and the hardening effect exceeds the softening effect. When the yield stress is reached, the curve slowly rises, the deformation enters the second stage, the work hardening rate gradually decreases, the internal dynamic recovery begins, and the softening offsets the partial work hardening. When the deformation enters the third stage, the curve gradually flattens out. In the stable rheological stage, work hardening is offset by a softening process caused by dynamic recovery. The rate of dislocation density increase caused by work hardening is almost equal to the rate of dislocation disappearance caused by cross slip and climb caused by dynamic recovery, and both reach dynamic equilibrium.

The corresponding fracture surfaces of the specimens are presented in Fig. 8. Comparison of the fracture surfaces of the specimens tested in nitrogen (Fig. 8a) or hydrogen (Fig. 5c) gas showed that hydrogen reduced significantly necking. Fig. 5a revealed also a strong anisotropy of the surface fracture under nitrogen atmosphere, related to the X80 microstructure anisotropy. To quantify the influence of hydrogen, an embrittlement index El was defined according to Eq. (1) where RN2 A and RH2 A respectively represented the reduction of area in nitrogen or hydrogen gas.

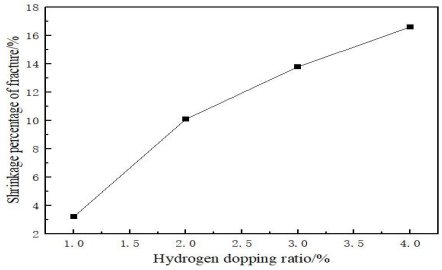

Figure. 5 . Shrinkage percentage of fracture in 20# pipeline steel with different hydrogen blending ratios.

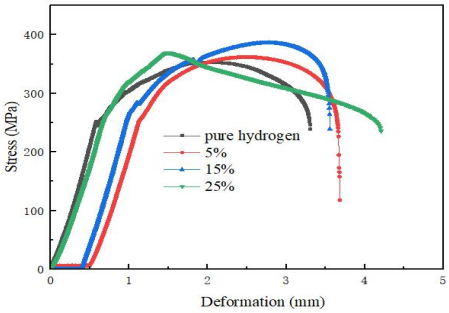

Figure. 6 Stress-deformation curves of 20# pipeline steel with different hydrogen blending ratios

Fig. 6 shows the stress-deformation curves of 20# pipeline steel measured after simulating different hydrogen mixing ratios, and the test environment of the comparison sample is the same pressure of 4MPa. It can be seen that in the elastic deformation stage, the stress-deformation curve trend of 20# pipeline steel under four test environments is generally consistent. Curves with a pure hydrogen and hydrogen-doped ratio of 25% rise from the beginning, while curves with 5% and 15% need to wait for a certain amount of deformation before they begin to rise.

The researchers believe that the hydrogen in the reversible hydrogen trap will lead to the hydrogen embrittlement of the material, but the hydrogen in the irreversible hydrogen trap is beneficial to improve the anti-hydrogen embrittlement ability of the material because it is not mobile. Hydrogen escaping from the material at a characteristic temperature below 300 ° C is considered diffusible, and hydrogen escaping above 300 ° C is considered nondiffusible[47-51]. The escape temperature and corresponding content of diffusible and nondiffusible hydrogen in the material can be measured by the thermal desorption instrument TDS.

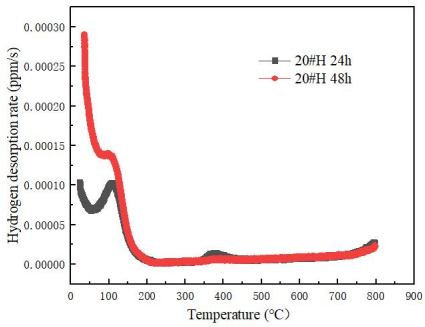

Figure.7 TDS curve of 20# pipeline steel after different hydrogen charging time.

The weld of 20# pipeline steel was processed into a Φ5×25 small cylinder, and the sample of the small cylinder was placed in the mixed solution of 0.1mol/L H2SO4 0.25g/L thiourea for electrochemical hydrogen charging. The hydrogen charging current was set to 5mA/cm2, and the hydrogen charging time was set to 24h and 48h respectively. Immediately after hydrogen charging is completed, the ultra-vacuum chamber of the TDS analysis equipment HTDS-003 is heated up to 800℃ at a heating rate of 100℃/h. The mass spectrometer of the equipment will record the change of the hydrogen desorption rate of the sample during the heating process.

The samples were charged with hydrogen in electrolyte under the same conditions (aqueous solution of 0.1 mol/L dilute sulfuric acid +0.25 g/L thiourea with a current density of 5 mA/cm2) for two different hydrogen charging times of 24 and 48h, and TDS analysis was performed immediately after. Figure 7 shows the desorption spectrum of hydrogen in the weld of 20# pipeline steel with increasing temperature. It can be seen that there is the same trend in the two desorption spectra, and there is a same desorption peak corresponding to 105˚C. There is also a less obvious desorption peak with a temperature of 374℃. Desorption temperatures below 300˚C are considered to be the desorption temperature of hydrogen in a reversible hydrogen trap, and peaks above 300˚C are considered to be the desorption process of

hydrogen in an irreversible trap. Therefore, there are both reversible and irreversible hydrogen traps in the internal structure of 20# pipeline steel.

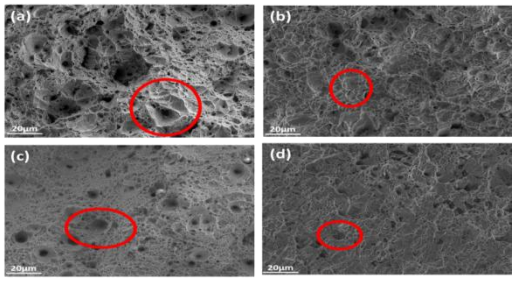

Figure.8 SEM morphologies of the fracture of the 20# pipeline steel with different hydrogen blending ratios:(a)5%;(b)15%;(c)25%;(d)100%

Moreover, Fig. 8a and c showed delamination on the fracture surfaces, but hydrogen enhanced this type of damage. Dealing with the fracture mode, Fig. 8b and d logically showed a ductile fracture with dimples in nitrogen gas (Fig. 8b) and a quasi-cleavage fracture mode in hydrogen gas (Fig. 8d). In addition, examination of the gage length external surface of the specimens loaded in hydrogen gas showed circumferential cracks rather homogeneously distributed.

All these features tended to prove that hydrogen induced two main damage modes. The first one, located in the bulk of the specimens, occurred by decohesion at the interface between pearlite alignments and ferrite matrix, easily visible on the fracture surface of the samples loaded in hydrogen gas (Fig. 8c). The second one, located at the surface of the specimen, consisted in brittle circumferential cracks, perpend.

By observing the macro morphology of the slow tensile fracture side of the smooth test steel, it is found that the fracture side of the sample with low hydrogen content ratio shows obvious necking and 45° shear lip characteristics, and the zigzag section shows typical tearing characteristics, while the fracture side appearance of the pure hydrogen content ratio is relatively flat, and no obvious necking characteristics are seen. Sievert equation [52] -degree can be used to explain the reason why hydrogen embrittlement degree increases with the increase of hydrogen content in the environment. As shown in Equation 2.5, a higher volume fraction of hydrogen in the environment corresponds to a higher partial pressure of hydrogen. It can be seen from the equation that the hydrogen concentration in the metal is proportional to the square root of the hydrogen pressure, so a higher partial pressure of hydrogen promotes a higher concentration of hydrogen in the metal, resulting in a more obvious hydrogen embrittlement.

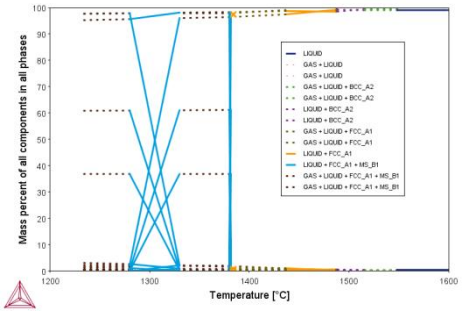

Figure. 9 Possible hydrogen forms in the 20# pipeline steel under working condition: Fe-0.20C-0.24Si-0.45Mn-0.020P-0.010S-0.010Al-0.0010H in mass pct. (Thermo-Calc software)

Since the effect of hydrogen on hydrogen embrittlement is caused by the generation of hydrogen-containing gas products, in order to explain the gas products, this paper attempts to use Thermo-Calc software to carry out relevant calculations. The Solidification process of 20# steel containing 10ppm hydrogen was calculated by the Scheil Solidification Simulation module of Thermo-Calc software. As can be seen from Figure 14, hydrogen is only a gas form and has no specific chemical formula, so it can only be simulated by other software.

Equilib is one of the most commonly used modules in FactSage software. It uses the Gibbs free energy minimization method to calculate the state of chemical equilibrium of a given element or compound under certain conditions (defined by temperature, pressure, etc.), including the concentration of each species.

In this paper, FactSage 8.1 version is used to calculate the various forms of hydrogen in 20# pipeline steel with different H content. The H content is set in the range of 2ppm to 10ppm, with an interval of 2ppm. It can be seen from Figure 15 that the possible forms of hydrogen in the 20# pipeline steel are H2S, H2, H, CHP, CH4 and C2H2. H2S increases with the increase of hydrogen content. When the content of H is 2ppm, the H2S content is 1.0315*10-8mol, and when the content of H is 10ppm, the H2S content increases to 5.283*10-8mol. H2 increases with increasing hydrogen content. When the H content is 2ppm, the H2 content is 9.5939*10-5mol, and when the H content is 10ppm, the H2 content increases to 4.9144*10-4mol. H increases with the increase of hydrogen content. When the H content is 2ppm, the H content is 2.7335*10-8mol, and when the H content is 10ppm, the H content increases to 1.4002*10-7mol. CHP increases with the increase of hydrogen content. When the content of H is 2ppm, the CHP content is 2.6766*10-8mol, and when the content of H is 10ppm, the CHP content increases to 1.3691*10-6mol. CH4 increases with the increase of hydrogen content. When the H content is 2ppm, the H content is 7.5434*10-8mol, and when the H content is 10ppm, the CH4 content increases to 3.864*10-7mol. C2H2 increases with the increase of hydrogen content. When the H content is 2ppm, the H content is 1.542*10-8mol, and when the H content is 10ppm, the H content increases to 7.8985*10-8mol. The change trend of the above six products is the same. In summary, the contents of H2S, H2, H, CHP, CH4 and C2H2 increased with the increase of H content, respectively, which promotes the possibility of hydrogen embrittlement of 20# pipeline steel.

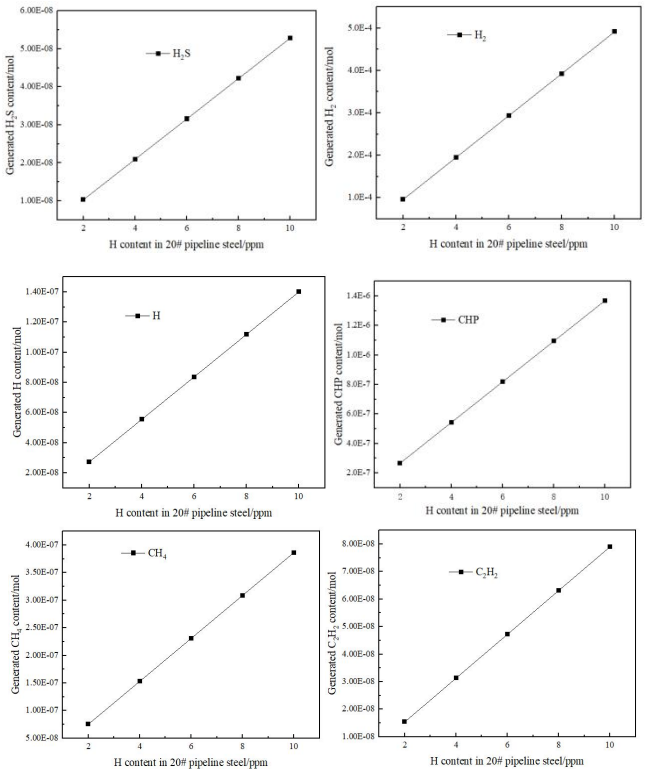

Figure. 10 Possible hydrogen forms in the 20# pipeline steel under working condition

Fe-0.20C-0.24Si-0.45Mn-0.020P-0.010S-0.010Al-<A>H in mass pct. (FactSage 8.1 software)

4. CONCLUSIONS

When 20# pipeline steel is directly exposed to a hydrogen containing environment and subjected to hydrogen intrusion from mechanical loads, metal HE may occur. Therefore, our research focus is on the impact of hydrogen produced from renewable energy on pipeline steel, in order to achieve large-scale transportation of existing natural gas pipelines. The

mechanical properties of 20# pipeline steel were tested in a simulated hydrogen /natural gas mixture of 5.0, 15.0, 25.0, and 100.0vol% hydrogen at a pressure of 10 MPa. The main conclusions are as follows:

(1) The hydrogen blending ratio plays an important role in the HE of 20# pipeline steel. The HE sensitivity indices tensile strength and reduction of area corresponding to the tensile test gradually increase, and with the increase of hydrogen, the propagation of fatigue cracks significantly accelerates.

(2) The trend of desorption spectra at 24h and 48h is the same, and there should be a same desorption peak at 105℃. The current experiment shows that the main internal structure of 20# pipeline steel is reversible hydrogen trap.

(3) The possible gas products of hydrogen embrittlement in 20# steel were proved by factsage software.

5. REFERENCES

[1] S.P. Trasatti, E. Sivieri, F. Mazza, Mater. Corros. 56 (2005) 111-117.

[2] N. Eliaz, A. Shachar, B. Tal, D. Eliezer, Eng. Fail. Anal. 9 (2002) 167-184.

[3] Bockris JOM, Veziroglu TN. Estimates of the price of hydrogen as a medium for wind and solar sources. Int J Hydrogen Energy 2007;32: 1605e10

[4] Du, Y. , et al. "Hydrogen Embrittlement Behavior and Mechanism of Low Carbon Medium Manganese Steel Gas Metal Arc Welding Joints." JOM 75.10(2023):4407-4420.

[5] H.K. Birnbaum, P. Sofronis, Mater. Sci. Eng. A176 (1994) 191-202.

[6] H.K. Birnbaum, Scripta Metall. Mater. 31 (1994) 149-153.

[7] S.P. Lynch, Met. Forum 2 (1979) 189-200.

[8] S.P. Lynch, Proceedings NACE International Conference Corrosion 2007, 2007 (paper 07493). [8] P.J. Ferreira, I.M. Robertson, H.K Birnbaum, Acta Mater 46 (1998) 1749-1757.

[9] Wu S , Gao Z , Liu Y ,et al.Effect of cathodic protection potential on stress corrosion susceptibility of X80 steel[J].Corrosion Science: The Journal on Environmental Degradation of Materials and its Control, 2023. 1-11

[10] P. Sofronis, Y. Liang, N. Aravas, Eur. J. Mech. A: Solids 20 (2001) 857-872.

[11] D.P. Abraham, C.J. Altstetter, Metall. Mater. Trans. 26A (1995) 2849-2858.

[12] B. Ladna, H.K. Birnbaum, Acta Metall. 35 (1987) 1775-1778.

[13] I. Moro, Ph.D. Thesis, University of Toulouse III, 2009.

[14] J. Chene, A.M. Brass, Scripta Mater. 40 (1999) 537-542.

[15] J.A. Donovan, Metall. Trans. 7A (1976) 1677-1683.

[16] J. Tien, A.W. Thompson, I.M. Bernstein, R.J. Richards, Metall. Trans. 7A (1976) 821-828.

[17] J.P. Hirth, Metall. Mater. Trans. 11A (1980) 861-890.

[18] J.P. Hirth, H.H. Johnson, in: R.A. Latanision, J.R. Pickens (Eds.), Atomistics of Fracture, Plenum Press, New York, 1983, pp. 771-785.

[19] S.V. Nair, R.R. Jensen, J.K. Tien, Metall. Trans. 14A (1983) 385-393.

[20] A.H.M. Krom, R.W.J. Coers, A. Bakker, J. Mech. Phys. Solids 47 (1999) 971-992.

[21] A.H.M. Krom, H.J. Maier, R.W.J. Koers, A. Bakker, Mater. Sci. Eng. A27 (1999) 22-30.

[22] R.A. Oriani, Acta Metall. 18 (1970) 147-157.

[23] A.J. Kumnick, A.H. Johnson, Acta Metall. 28 (1980) 33-39.

[24] G.M. Pressouyre, I.M. Bernstein, Metall. Trans. 9A (1978) 1571-1580.

[25] Yao, Weijing , et al. "Study on mechanical properties and damage characteristics of rubber concrete under equal amplitude high stress repeated loading." Journal of Material Cycles and Waste Management (2023).

[26] A.M. Brass, J. Chêne, J. Coudreuse, Technique de l' Ingénieur M176.

[27] I. Moro, L. Briottet, P. Lemoine, E. Andrieu, C. Blanc, G. Odemer, J. Chêne, F. Jambon, Proceedings of the 2008 International Hydrogen Conference on Effects of Hydrogen on Materials, Jackson Lake Lodge, Wyoming, USA, 2008.

[28] L. Coudreuse, P. Neumann, Application des critères de mécanique de la rupture aux matériaux ductiles chargés en hydrogène, Commission Européenne Recherche Technique acier, EUR 17872, 1998.

[29] H.L. Eschbach, F. Gross, S. Sculien, Vacuum 13 (1963) 543-547.

[30] H.K. Birnbaum, I.M. Robertson, P. Sofronis, D. Teter, Eur. Fed. Corros.Publ. 21 (1997) 172-195. [31] D.G. Ulmer, C.J. Altstetter, Acta Metall. Mater. 39 (26) (1991) 1237-1248.

[31] I.M. Robertson, Eng. Fract. Mech. 68 (2001) 671-6921.

[32] Dwivedi SK, Vishwakarma M. Hydrogen embrittlement in different materials: a review. Int J Hydrogen Energy 2018;43:21603e16.

[33] S.K. Dwivedi, M. Vishwakarma, Hydrogen embrittlement in different materials: a review, Int. J. Hydrogen Energy 43 (46) (2018) 21603-21616.

[34] Q. Liu, Q. Zhou, J. Venezuela, M. Zhang, A. Atrens, Hydrogen influence on some advanced high-strength steels, Corrosion Sci. 125 (2017) 114-138.

[35] M. Koyama, S.M. Taheri-Mousavi, H. Yan, J. Kim, B.C. Cameron, S.S. MoeiniArdakani, J. Li, C.C. Tasan, Origin of micrometer-scale dislocation motion during hydrogen desorption, Sci. Adv. 6 (23) (2020).